Molecular dynamics simulation of tensile elongation of carbon nanotubes: Temperature and size effects

Chun Tang,[1,2] Wanlin Guo,[1,2] and Changfeng Chen[1]
[1]*Department of Physics and High Pressure Science and Engineering Center, University of Nevada, Las Vegas, Nevada 89154, USA*
[2]*Institute of Nano Science, Nanjing University of Aeronautics and Astronautics, Nanjing 210016, China*
(Received 19 April 2008; revised manuscript received 23 March 2009; published 23 April 2009)

We report molecular dynamics simulations of tensile elongation of carbon nanotubes (CNTs) over a wide temperature range. In particular, we examine temperature and size effects on tensile ductility of CNTs and compare our results with recent experimental observation on superplastic deformation of CNTs at high temperatures. Our simulations produce substantial tensile ductility in CNTs with large diameters at high temperatures and reveal that similar behavior can be realized over a surprisingly large temperature range between 500 and 2400 K that is yet to be fully explored by experiments. At lower temperatures, tensile deformation modes become brittle due to defect localization attributed to insufficient thermal energy for wide distribution of defect nucleation. For CNTs with smaller diameters, our simulations produce strong defect localization which leads to brittle behavior even at high temperatures. Sensitive dependence on the distribution of incipient defects on thermal energy results in a significant decrease in the elastic limit with increasing temperature. We propose an effective tensile ductility enhancement via temperature reduction beyond the elastic limit. The results offer insights for understanding intriguing temperature effects on tensile deformation modes of CNTs.

DOI: 10.1103/PhysRevB.79.155436 PACS number(s): 61.46.Fg, 62.20.fq, 62.25.−g

I. INTRODUCTION

Carbon nanotubes (CNTs) exhibit exceptional mechanical properties.[1–4] Among the fundamental issues are their elastic and plastic deformation behaviors under tensile loading and the associated breaking and failure modes. Previous theoretical studies[4,5] show that the critical failure strain of CNTs under tensile loadings is no more than 20%, while in early experiments only 6% was achieved for single-walled CNTs (SWCNTs) (Refs. 6 and 7) and 12% for multiwalled CNTs.[3] However, recent experiments[8,9] performed at high temperatures (about 2 000 °C) revealed surprisingly larger (typically over 50%) superplastic deformation behavior in CNTs with large tube diameters. These results present a challenge to the existing understanding on the mechanical properties of CNTs, especially their deformation modes at different temperatures and tube sizes.

Several pioneering theoretical works have been reported by Yakobson and co-workers on the onset of plastic deformation in CNTs at high temperatures.[10,11] They pointed out that the plastic elongation could be achieved by the so-called Stone-Wales transformation, i.e., the nucleation of pentagon-heptagon pairs from the well defined hexagonal graphite network via a 90° rotation of a C-C bond. To facilitate large plastic elongation, high-temperature condition along with tensile strain is essential for providing external energy to overcome the energy barrier for defect nucleation and motion.[10–12]

While previous results provide important insights into the mechanism of nucleation of the topological defects responsible for plastic elongation, several fundamental issues concerning tensile deformation of CNTs remain to be explored. Most of existing theoretical studies focused on short segments of CNTs with very small diameters. They are used in conjunction with engineering modeling analysis to demonstrate the principles for the nucleation of a single topological defect and its subsequent motion on the tube wall. However, these results do not provide an adequate description for the generation, distribution, and interaction of a large number of defects present in realistic CNTs with larger sizes. In recent experiments,[8] the observed superelongation occurs in CNTs with large diameters up to 12 nm, followed by significant reduction in diameter before eventual breaking of the tube. Another experiment showed that the inner most tube wall of a triple-walled CNT breaks first.[9] These results suggest that CNTs with large diameters are more ductile, which is in stark contrast to early theoretical prediction that CNTs with small diameters are favored for plastic elongation.[10] Therefore, the dependence of tensile ductility of CNTs on the tube size should be re-examined. Furthermore, in the reported experiments, it is noted that multiple defects and kinks were generated during the elongation process. As a result, the interaction among the defects becomes inevitable and is expected to play an important role in the deformation process. It is, therefore, necessary to go beyond the previously considered scenario of ideal glide of a single defect on the tube wall[10,13,14] and to examine in detail the complex dynamic behavior of multiple defects on CNTs. Another important issue concerns the range of temperatures where large plastic deformation can be produced in CNTs. Previous studies were conducted either at room temperature or at high temperatures around 2 000 °C. It would be interesting to examine the response of CNTs subjected to tensile loading at intermediate temperatures. The results are expected to shed light on the role of temperature in producing the superplastic behavior and the interplay between the thermal energy and the mechanical strain energy during the elongation process.

In this paper, we report molecular dynamics (MD) simulations on tensile deformation of SWCNTs at temperatures ranging from 300 to 2400 K. Previous results show that, regardless of their starting chiralities, SWCNTs will eventually evolve toward zigzag type.[10] We therefore focused on

zigzag SWCNTs in this study. We found that tensile ductility can be achieved in CNTs with large diameters [greater than that for the (31,0) SWCNT] over a surprisingly large temperature range (500–2400 K). Our results also reveal sensitive temperature dependence of the elastic limit of SWCNTs over a broad range of diameters, in agreement with previous simulation evidence.[16,17] Furthermore, it is shown that tensile deformation modes of SWCNTs at high temperatures and lower temperatures are different because of the different roles played by the thermal and strain energy. The interplay of these different roles leads to an intriguing enhancement of tensile ductility of CNTs by temperature modulation during the elongation process.

II. METHODS

The second-generation reactive empirical-bond-order potential was adopted in the present simulation. It was developed for hydrocarbons on the basis of Tersoff-Brenner expression. The *L-J* potential in the form of

$$V(r_{ij}) = 4\varepsilon\left[\left(\frac{\sigma}{r_{ij}}\right)^{12} - \left(\frac{\sigma}{r_{ij}}\right)^{6}\right]$$

describing the long-range van der Waals interaction was also included,[18,19] where the *L-J* constants used in our simulations are $\varepsilon=51.2$ K and $\sigma=2.28$ Å. The Berendsen thermal scheme[20] was used to control the temperature at a constant value. In comparison with other computational approaches, such as Monte Carlo (MC) simulations that use statistical sampling algorithm to obtain system configurations and thus do not provide real-time dynamic process or large-scale quantum mechanical calculations that are prohibitively expensive in computing costs, the MD simulation approach has the advantage of providing reasonably accurate descriptions at acceptable computational costs. It has been widely adopted as a leading computational method in the study of atomistic behavior of large size material systems and has produced accurate descriptions for structural evolution of carbon systems including C-C bond compression, stretching, rotation, and bending, as well as lattice twisting of carbon nanotubes.[21–27] In particular, this method has been proven to be capable of describing the nucleation of topological defects such as the Stone-Wales transformation responsible for plastic elongation of CNTs at high temperatures.[10] It is noted that this potential produces unphysical results at cutoff bond lengths between 1.7–2.0 Å,[28–30] and several groups have made certain modifications to avoid such problems.[29,31,32] We will show below that, in the present work, this flaw is largely avoided since the bond length stays below the above-mentioned cutoff bond length range at high temperatures. Considering that the Stone-Wales defect activation energy barrier from quantum mechanical calculations varies in a large range from 8.5 to 10.4 eV or even beyond,[12,13,33,34] the energy barrier from Tersoff-Brenner potential of approaching 10 eV (see also, for example, Ref. 17) is acceptable.

In this paper we primarily focus on results for SWCNTs with diameters ranging from 0.63 nm for the (8,0) tube to 4.7 nm for the (60,0) tube at the same length of 10.6 nm. For the effect of tube length variation, we performed a comparative case study of two (10,0) SWCNTs with the same diameter but different lengths; the results show that they exhibit similar local deformation patterns although there are significant differences in the extent of total tube elongation. In our simulations, tensile loading was realized by keeping one end of the tube fixed while adding an axial displacement to the other end at the loading rate of 0.08 Å per 4000 fs, which is the lowest rate compared to other existing computer simulations on tensile loading of one-dimensional nanomaterials with similar system size.[35–38] We have also performed simulations at lower loading rate (0.08 Å per 5000, 10 000, and 20 000 fs) and found the same trend in tensile deformation modes as obtained at the loading rate of 0.08 Å per 4000 fs. It should be noted, however, that the strain rate in our simulations is about 10 orders of magnitude higher than that in the reported experiments, which is expected to have a major influence on the physics studied here.

III. RESULTS AND DISCUSSION

We recently carried out extensive molecular dynamics simulations of tensile elongation of carbon nanotubes and examined the atomistic deformation modes at high temperatures. It was shown[39] that the experimentally observed superelongation of SWCNTs can be achieved at 2000 K and that nucleation and interaction of multiple defects near the elastic limit play a crucial role in producing the superplastic behavior. The results reveal rich and complex defect nucleation mechanism and plastic flow patterns beyond those reported in previous work. Here we further expand the scope of this work and address several issues concerning the effects of temperature and tube size on the tensile deformation of SWCNTs that are important to understanding their structural deformation behavior but still remain largely unexplored. We first examine the situation at higher temperatures above 2000 K and find that similar superplastic tensile deformation can be achieved in a wide range between 2000 and 2400 K, suggesting that the observed superplastic behavior is a common phenomenon at such high temperatures. At still higher temperatures above 2400 K, sublimation may become an increasingly important factor and, consequently, different mechanisms would probably have to be considered. In the present work, we consider the cases without sublimation for a consistent description for SWCNT elongation at high (up to 2400 K) and low (down to 300 K) temperatures.

We show in Fig. 1 our calculated strain energy and the corresponding structural evolution of a (31,0) SWCNT under tension at 2400 K, which is close to that estimated in experiments.[8,9] The results clearly demonstrate the tensile ductility of the (31,0) SWCNT at this high temperature. When the SWCNT is pulled over its elastic limit, a steep drop in strain energy occurs accompanied by widespread nucleation of a large number (hundreds) of topological defects on the tube wall. However, the tubular structure is initially well maintained and still capable of undertaking further tensile loadings. During the tensile elongation process, the tube shrinks in diameter due to the plastic flow of the defects. The critical (or breaking) strain at which the tube fails approaches 51%. These results are consistent with the ex-

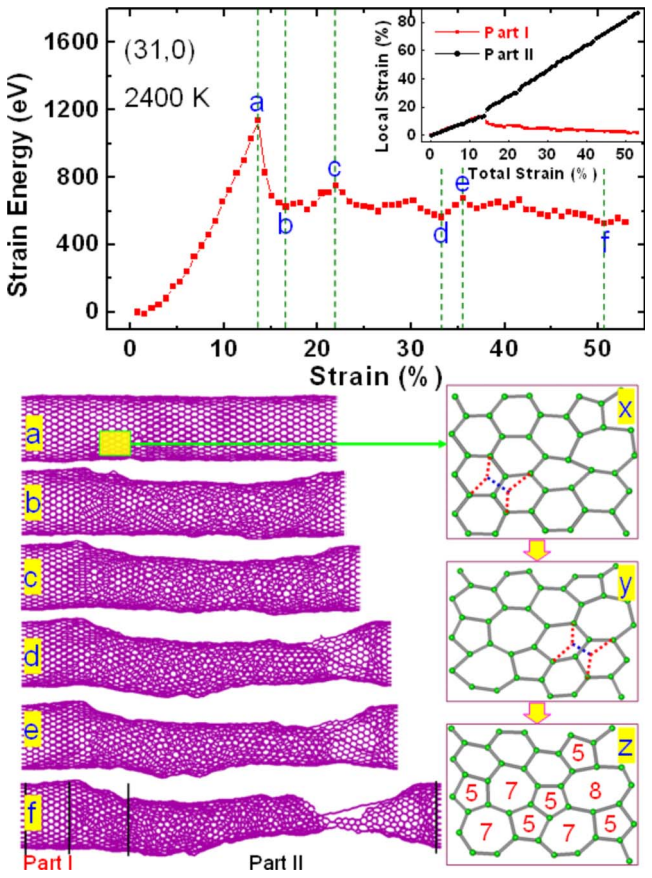

FIG. 1. (Color online) Strain energy (top panel) and structural evolution (bottom panels) of a tensile loaded (31,0) SWCNT at 2400 K. The SWCNT is 10.6 nm in length and 2.43 nm in diameter. The inset in the top panel shows the local strain of the elastic and plastic segments (part I and part II as denoted in configuration *f*) during the elongation process. Configurations $a-f$ are snapshots of the SWCNT structure taken from the simulation. Snapshots *x*, *y*, and *z* are atomic views of the defect nucleation and motion on the tube wall (from total strain level 13.8% to 14.1%). Nucleation of an octagon ring is clearly seen by the rotation of a "shoulder" bond of the heptagon ring. The dashed lines are schematic illustrations of the bond rotation and newly formed C-C bonds.

perimentally observed typical elongation (about 50%).[8] It is interesting to note that when a plastic segment of the tube (segment part II in Fig. 1) is measured, the local strain can reach a much higher value of 81%. Here we define the breaking strain of a CNT when a part of the tube wall is unraveled into atomic chains bridging two separated segments of the tube wall, as shown in Fig. 1(f); similar phenomenon has also been observed in previous MD simulations.[16,40] This criterion is consistently applied to all our simulations results reported in this paper. It is noticed that the strain energy undergoes several stages (separated by the vertical dashed lines in Fig. 1) of rising, falling, holding steady, and rising again before finally approaching the unraveling of the tube. Previous work indicated that the strain level and plastic flow of only a few Stone-Wales defects can affect the thermal energy[41] and the kinetic energy barrier[12,42] effectively. The CNTs in the present simulations contain a larger number of defects. The observed multistage fluctuation of strain energy reflects the complex interplay between the elastic and plastic segments and the plastic flow of the tube during tensile elongation.[39] Our simulations on CNTs with different diameters indicate that tubes with larger diameters are able to accommodate more stages of necking and kink motion, yielding larger elongation.

To gain insights into the mechanism for the tensile elongation behavior obtained in the simulations, we examine the atomistic processes associated with incipient defect nucleation and motion that occur shortly after the strain exceeds the elastic limit. Configurations *x*, *y*, and *z* in Fig. 1 show typical simulated structural snapshots of the initiation and development of the incipient defects on the tube wall of the (31,0) SWCNT between strain levels from 13.8% to 14.1%, i.e., slightly beyond the elastic limit. It is seen that the initial nucleation of the defect takes the form of the 90° rotation of a C-C bond, resulting in the Stone-Wales defects, which is consistent with previous predictions.[10,11] However, our simulations show that subsequent plastic flow of these defects does not follow the predicted ideal helical pathway.[10,14] Instead, it is seen clearly in Fig. 1 $(y-z)$ that due to the rotation of the C-C bond connecting to the heptagon ring, an octagon is also nucleated. Other defects such as the nonagon or even bigger defect rings were also observed in later stages of the simulated elongation process. Our results are in contrast to an earlier empirical prediction that the octagon rings are the source of brittle fracture,[11] which was later proven incorrect by a quantum mechanical calculation.[29] A recent experiment showed that even very large vacancy holes can be involved in plastic deformation of CNTs,[43] which is in good agreement with our simulation results. These results indicate that the interactions among the incipient Stone-Wales defects generate new types of defects and complicate their motion on the tube wall. Consequently, the kink can propagate in either a helical or a longitudinal pathway[15] due to the complex multiple defect interaction and motion. The large defects generated by these interactions eventually lead to the formation of big holes on the tube wall [Fig. 1(d)], as observed in recent experiment.[43] As a result, the local tube structure gradually unravels into carbon nanoribbons with the subsequent plastic flow restricted to a small segment in the vicinity of such a dominant defect localization.

At high temperatures, other types of incipient defects on CNT walls such as vacancies and/or larger holes[32,43,44] could be induced either by bond breaking or by atom evaporation.[8,45] These defects are expected to reduce the tensile strength of CNTs.[32,44] However, such defects are also expected to have strong self-healing ability and eventually evolve toward Stone-Wales type defects.[14,46,47] It is also noted that recent experiments showed that CNTs are thermally stable at temperatures up to 3200 K,[48] which suggests that the atomic evaporation mechanism requires further investigation, because large thermal fluctuations at temperatures over 3200 K will inevitably impede the proposed dynamic evolution along the ideal pathway.[14,46]

From the simulation results shown in Fig. 1 we can identify that when plastic deformation is initiated beyond the elastic limit of SWCNTs, a large number of defects are activated almost simultaneously over large segments of the tube wall. This is a common character observed in our simulations

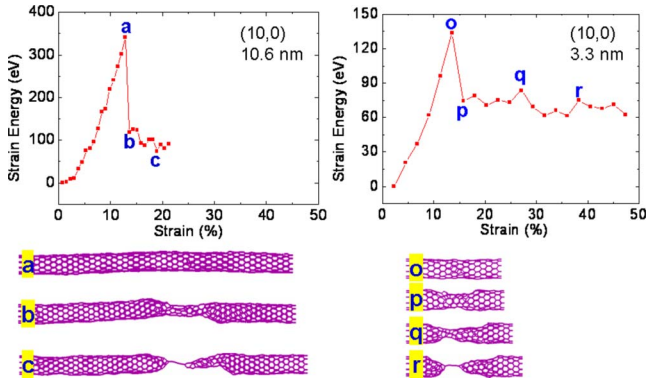

FIG. 2. (Color online) Tensile loading of the 10.6 and 3.3 nm (10,0) SWCNTs at 2000 K. Several key structural snapshots are shown in each case.

on SWCNTs that exhibit superplastic tensile elongation behavior. Without this favorable initial defect distribution, predominant defect localization would severely impede the motion of the defects into the structurally stronger defect-free segment and limit the overall plastic flow of the tube. This is illustrated by the snapshots shown in Fig. 1, where the leftmost segment of the tube wall retained its hexagonal networks throughout the elongation process due to a lack of initial defect nucleation in that segment. Once the initial defect nucleation occurs shortly over the elastic limit, strain energy is effectively released by the plastic flow in the defective segment of the tube, making it very difficult to induce additional defects in the defect-free segment which is stronger than its defective counterpart.[49] At the same time, the plastic flow around the defective area is energetically favorable because of its low energy cost.[10] The strain energy release also leads to significant C-C bond contraction, especially in the defect-free segment. It is noted that the CNTs that showed the most dramatic superplastic behavior in the reported experiments[8,9] have relatively short lengths compared to typical as grown tubes.[50,51] This choice helped to optimize the extent of the relative elongation by maximizing the ratio of the plastic segment of the tube. Use of longer tubes would probably reduce the extent of the overall elongation since it would be much more likely that the tube would contain some defect-free elastic segment given the statistical nature of thermal energy induced defect activation. This scenario was indeed seen in recent experiments on stretching metallic glass or nanowires.[52–54] It was shown that while the overall tensile strain of a SiC nanowire is about 28%, a measure of the local plastically elongated part yielded a superplastic strain of over 200% at room temperature. This phenomenon was explained by the homogeneously generated defects within the measured area,[54] which is consistent with the conclusions drawn from our simulations of the CNTs. To illustrate this point, we show in Fig. 2 calculated strain energy versus strain for a 10.6 and a 3.3 nm (10,0) SWCNT at 2000 K. It is clearly seen that the shorter (3.3 nm) tube exhibits much larger total elongation despite that the two tubes have nearly identical local plastic deformation.

We now turn to the influence of tube diameter on tensile deformation of SWCNTs. Recent experiments[8,9] showed that

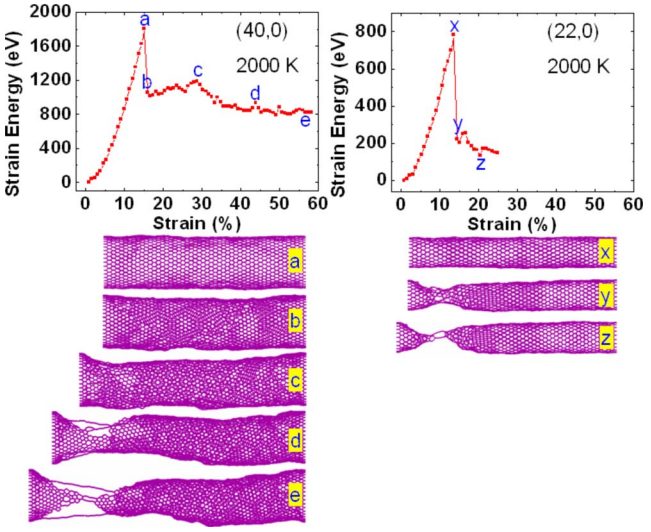

FIG. 3. (Color online) Tensile loading of the (40,0) and (22,0) SWCNTs at 2000 K. Configurations $a-e$ and $x-z$ are selected snapshots during the tensile elongation processes, as denoted in the strain energy plots.

CNTs with larger diameters are favorable for superplastic tensile elongation, but did not attempt to identify the lower limit of tube diameter for the superelongation behavior. Our simulations show that CNTs with larger diameters indeed exhibit larger tensile elongation under the same tensile loading conditions. It suggests that the energy barrier for defect activation on CNTs depends on the degree of tube wall curvature which is consistent with recent observation that binding energy of CNTs shows dependence on tube diameters.[55] To analyze this phenomenon, we examine the results for the (40,0) and (22,0) SWCNTs at 2,000 K shown in Fig. 3. For the (40,0) tube, when it is stretched over the elastic limit nearly homogeneous defect nucleation occurs, resulting in the large tensile ductility. Meanwhile, for the (22,0) tube, defects are strongly localized and the overall elongation process is brittle. Our systematic simulations of a large number of SWCNTs indicate that tensile ductility occurs in tubes with diameters greater than that (2.35 nm) of the (30,0) tube. For tubes with smaller diameters, initial defect nucleation is localized. In addition to the curvature dependence of the defect activation energy mentioned above, it is also noted that a small number of defects can lead to a relatively high defect concentration and significantly affect the stiffness of the SWCNT within a local area. To evaluate the temperature effect on this phenomenon, tensile loading at room temperature (300 K) was also studied. Results in Fig. 4 show clear brittle breaking pattern even for the larger (40,0) tube. However, it should be mentioned that brittle breaking modes are also accompanied by activation of topological defects; but unlike defects nucleated at high temperatures these defects are strongly localized due to a lack of sufficient thermal energy. This can be seen in the tensile loaded (40,0) tube at 300 K: after being stretched over its elastic limit, a short segment of the tube necks dramatically, but the tubular structure remains intact over a transition regime before the tube finally broke. Nevertheless, the overall behavior is brittle because the plastic defect flow restricted within the necked segment

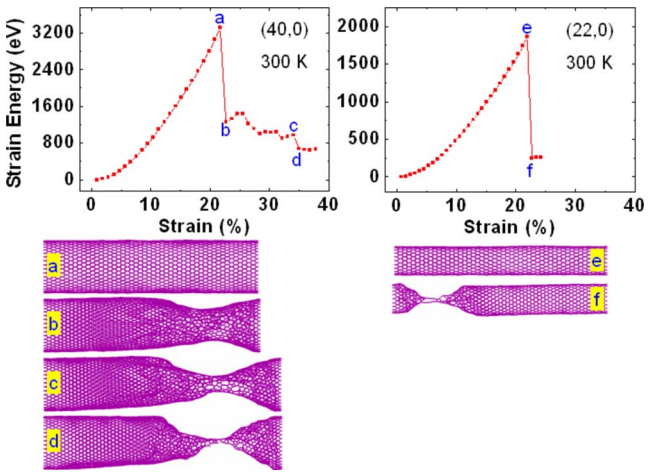

FIG. 4. (Color online) Strain energy and structural evolution of the (40,0) and (22,0) SWCNTs under tension at 300 K.

is visibly weak due to the lack of thermal energy. For SWCNTs with smaller diameters, there is less room for necking at the locally damaged tube wall. When the diameter is sufficiently small (such as the case for the (22,0) tube), a direct breaking of the tube occurs when it is stretched over the elastic limit, as shown in Fig. 4(b).

Previous experimental and theoretical studies focused on plastic elongation of CNTs at temperatures over 2000 K. It would be interesting to investigate whether tensile ductility can be produced at lower temperatures. Since the reported experiments did not have precise control over temperature during the measurement, a theoretical study can provide useful insights into the underlying mechanisms. We conducted simulations on tensile loading of SWCNTs over a wide temperature range. Figure 5 shows the results of the (31,0) tube at several different temperatures. It is seen that the maximum broken strains are 42%, 36%, and 34% at 1200, 900, and 500 K, respectively. Nucleation of defects and their subsequent motion lead to the shrinking of the tube wall, demonstrating that the tube is ductile at these intermediate temperatures. At temperatures below 500 K, defects on the wall of the (31,0) tube are localized and the overall elongation becomes brittle, which can be attributed to the lack of thermal energy at the

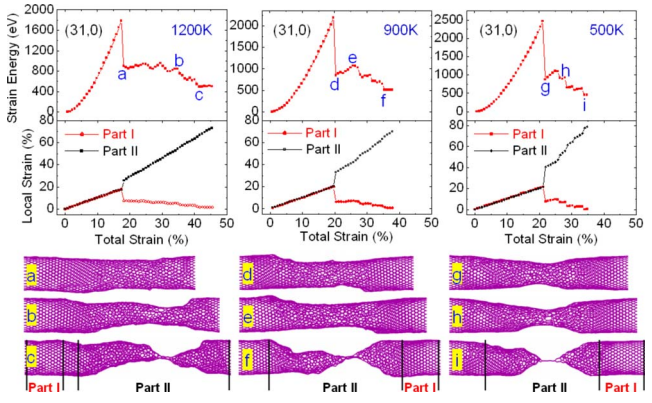

FIG. 5. (Color online) Strain energy, local strain and structural evolution of a tensile loaded (31,0) SWCNT at different temperatures.

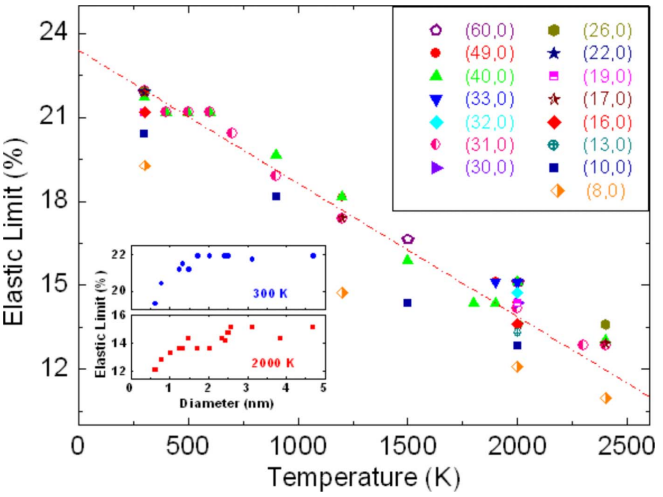

FIG. 6. (Color online) Temperature dependence of elastic limit of SWCNTs under tensile loadings. The insets on the lower-left corner show the elastic limit at 300 and 2000 K, respectively, for SWCNTs with different diameters. Symbols representing different SWCNTs are indicated in the panel on the upper-right corner. The dash-dotted line is a guide to the eyes.

reduced temperatures similar to the situation at room temperature discussed above. We also measured local strains of the elastic (containing no defects) and plastic segments of the tube as shown in Fig. 5. These local strains start to diverge beyond the elastic limit, reflecting the distinct characters of their respective deformation modes. They provide a more detailed and informative description for the elongation of different tube segments compared to what can be learned from the overall strain. Our simulations show that for SWCNTs with diameters greater than that of the (30,0) tube tensile ductility can be achieved over a wide temperature range. For example, our simulations show that the (40,0) tube can be plastically stretched to breaking strain of 68%, 51%, and 37% at 2400, 900, and 500 K, respectively. It is noted that several previous works showed that the ultrastiff description of C-C bond at 1.7–2.0 Å by the Tersoff-Brenner potential would lead to unphysical behavior of CNTs under tensile loading.[28–30] However, this flaw does not influence the conclusions we draw in this paper. This is because our simulations were mainly conducted at high temperatures where the elastic limit of CNTs is relatively low as shown in Fig. 6. For example, at 2000 K, the elastic limit of all zigzag SWCNTs saturates at 15%, corresponding to maximum C-C bond length of 1.62 Å in circumferential direction and 1.52 Å in axial direction, which are well below the cutoff of 1.7 Å. An examination of our calculated results shows that this cutoff is not reached at temperatures above 500 K (corresponding to maximum bond length of 1.697 Å). While at room temperature, our results show that CNTs are primarily brittle although the maximum bond length slightly exceeds 1.7 Å.

While tensile ductility is generally observed in SWCNTs with large diameters over a wide range of temperatures, there are some differences in the details of their deformation modes as temperature changes. From results shown in Fig. 5 and Fig. 1, two characteristic features are noticed: first, the

maximum broken strain decreases with decreasing temperature as described above; and second, the critical strain for the onset of plastic deformation (i.e., the elastic limit) varies with temperature. For the (31,0) tube, the elastic limit increases from 13% at 2400 K to 21% at 500 K. We have examined this behavior for a large number of SWCNTs at many temperature points and summarized the results in Fig. 6. It is clear that all the SWCNTs examined here show nearly universal linear decreasing trend in their elastic limit with increasing temperature regardless they are ductile or brittle. This phenomenon can be attributed to the interplay of the two main sources for defect nucleation, namely, the thermal energy and the strain energy, both of which are important to the defect nucleation and motion that are responsible for the plastic elongation of SWCNTs.[12,39] At higher temperatures, the system would require less energy from tensile loading to activate the defects compared to the lower-temperature cases and, therefore, the elastic limit is lower. The almost linear relationship can be attributed to the linear dependence of thermal energy on temperature. Beyond the elastic limit, tensile strain energy is effectively released and thermal energy plays a dominant role in the plastic deformation process. This explains the observation of the simulated results that tensile ductility is enhanced for the same tube at higher temperatures since plastic flow becomes easier compared to the situation at lower temperatures. Previous work on small-diameter SWNTs showed a similar trend;[16,17] the present work demonstrates that this trend remains valid for a larger variety of SWNTs. A recent tight binding calculation showed that the bond breaking strain of SWCNTs in tension decreases with increasing temperature,[56] which is similar to our conclusion, although it should be noted that the bond breaking strain is different from the elastic limit. In another recent theoretical work, Zhu *et al.*[57] showed that in a uniaxially compressed Cu nanowire, the surface dislocation nucleation stress decreases monotonically with temperature, which is also similar to our results.

Our simulations also reveal a scaling trend for the elastic limit of SWCNTs with their diameters. The insets in Fig. 6 show the results for a large number of SWCNTs at 300 and 2000 K, respectively. It is seen that at both lower and higher temperatures the elastic limit initially increases monotonically with increasing tube diameter; at further larger tube diameters, this trend weakens and the elastic limit approaches a saturation value of about 22% and 15%, respectively. We also conducted simulations on a graphene sheet unraveled from a (31,0) SWNT, the calculated results show that the elastic limit of this graphene is 21.5% at 300 K and 15% at 2000 K, respectively, suggesting that the same saturation trend holds for zigzag SWNTs with all possible curvatures. It should be noted that although the graphene sheet simulated here exhibits the plastic deformation mode at 2000 K, it is not sufficient to mimic the plastic behavior of an infinite SWNT because the width of the structure is very limited so that the edge effect cannot be neglected. The same trend is observed in our simulations at other temperatures although data points are not as dense. This phenomenon can be attributed to the high curvature of the SWCNTs with small diameters in its circumferential direction. It induces strong pre-existing strain energy in the tube and, hence, requires less tensile strain energy for the onset of plasticity. As a result, mechanical properties of small-diameter SWCNTs such as the Young's modulus is inferior compared to those with larger diameters[58] that are structurally closer to the unrolled planar graphite sheets in geometry. Our results are also consistent with a previous quantum mechanical calculation that reported that zigzag SWCNTs with diameters smaller than that of the (12,0) tube exhibit decreasing elastic limit with decreasing tube diameter.[13]

The finding that the elastic limit of a SWCNT under tensile loadings decreases with increasing temperature has important implications. For a SWCNT elongated at high temperatures, a reduction in its temperature would reduce the extent of defect nucleation due to the decreased thermal energy. It would improve the structural integrity of the tube by preventing early formation of large, dominant defects on the tube wall and, consequently, extending the plastic flow of the tube. This suggests a scenario for a self-enhancing plastic elongation mechanism for SWCNTs at high temperatures under the experimental heating scheme[8,9] that used Joule heating to produce the high-temperature conditions by applying a constant voltage across the tube ends. It was observed that when the CNTs are plastically deformed, the measured current decreases due to the scattering by the structural defects (see supplementary information of Ref. 8), which is expected to lead to decreasing temperatures experienced by the tube after the onset of the plastic deformation. Therefore, the Joule heating procedure employed in the experiments[8,9] not only provided the high-temperature environment for the CNTs, but also generated a perhaps unintended self-enhancing mechanism for improved tensile ductility in CNTs. This expectation is corroborated by our simulations presented below.

In Fig. 7 we present several typical cases of tensile ductility enhancement via temperature modulation by a slight reduction in temperature beyond the elastic limit, where the largest drop in current-induced heating is expected to occur. Significant improvement in tensile ductility is clearly visible. In particular, it is noticed that the tubular structure is significantly better retained when the temperature drops after the elastic limit. We have varied the magnitude of the temperature modulation beyond the elastic limit and examined other SWCNTs with different diameters and obtained similar results. In general, tubular structural integrity and broken strain are improved by this self-enhancing mechanism, which can be attributed to the increasing elastic range with decreasing temperature. In some cases, the overall tensile strain can be extended dramatically, as in the case of the (40,0) tube at 1800 K shown in Fig. 7(d) where tensile elongation improved from below 50% to over 70%. Meanwhile, our simulations show that this self-enhancing mechanism does not work at lower temperatures. For example, for the (31,0) tube at temperatures below 900 K, our simulations found little enhancement in tensile ductility via temperature modulation beyond the elastic limit. This is because at lower temperatures, strain energy plays a dominant role in defect nucleation, which tends to be more concentrated compared to the situation at high temperatures when large thermal energy produces wide distribution of incipient defects. The different mechanism at lower temperatures impedes the plastic flow of

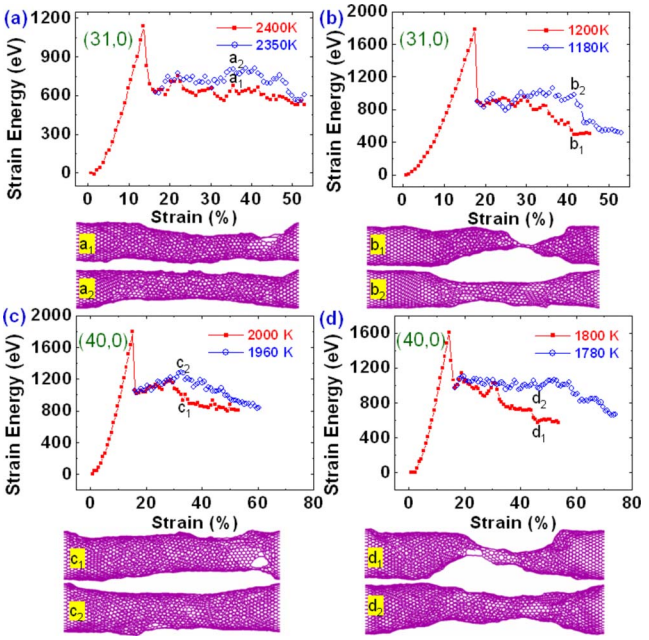

FIG. 7. (Color online) Tuning tensile ductility of the (31,0) and (40,0) SWCNTs via reducing temperatures. a_1-d_1 are snapshots from simulation at constant temperatures; a_2-d_2 are the corresponding structures (with the same tensile strain) obtained with temperature tuning.

the tube and makes its deformation more brittle.

We also explored the possibility of multiple stages of temperature reduction during the tensile deformation, considering that in the experiments the current decreases continuously with the elongation process.[8,9] We have performed simulations with multiple-stage temperature reduction on several SWCNTs with different diameters and observed various degrees of improvement in their tensile ductility. Since the reported experimental work did not have precise temperature control, a quantitative comparison between the measured and simulated results is not feasible at this point. It is not our purpose here to reproduce the yet unknown temperature variation in actual experimental situations. Instead, we attempt to demonstrate in principle significant effects of temperature modulation on the tensile ductility of CNTs and to reveal rich structural responses in such processes. In Fig. 8 we show, as a typical example, the results for the (32,0) tube tensile loaded at 2000 K, first without and then with temperature modulation beyond the elastic limit. Without any temperature reduction beyond the elastic limit, the overall broken strain is 42% as shown in Fig. 8(a). We then examined a one-stage and two different two-stage temperature reduction schemes. In all the cases, significant improvement in tensile ductility is achieved. There is a considerable expansion in the strain range between the elastic limit and the next steep drop in strain energy which signals large deterioration in structural integrity. In the scenario shown in Fig. 8(d), the broken strain is extended to 60% from the original 42%. Improvement in the load bearing ability of the tube at larger strains is also clearly visible. These results demonstrate that the plastic elongation behavior of CNTs could be successively enhanced via continuous temperature reduction in the experimentally

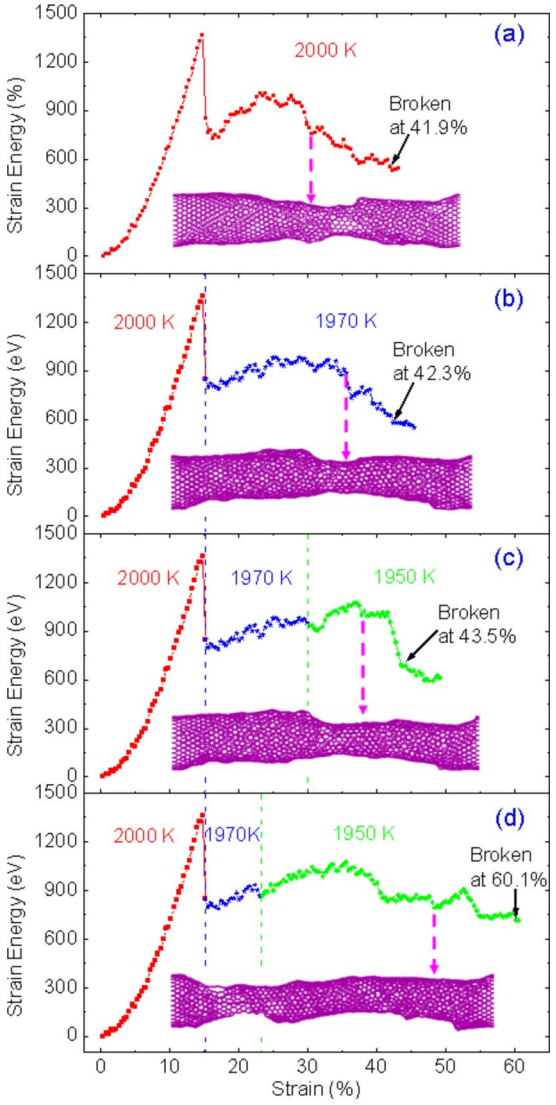

FIG. 8. (Color online) Enhancement of tensile ductility of a (32,0) SWCNT through successive temperature reduction beyond the elastic limit. Selected structural snapshots of the elongated tube are shown in each panel at the strain indicated by the thick dashed-line arrow.

employed Joule heating scheme.[8,9] The present results raise intriguing prospect for improving tensile ductility of CNTs via temperature modulation, which may stimulate further studies of this phenomenon and lead to better understanding of temperature control of tensile plasticity of CNTs and possibly other tubular structures.

Finally, we discuss the statistical nature of the defect nucleation on CNTs at high temperatures observed in our simulations. While large tensile ductility is a general behavior at high temperatures, formation of dominant defect nucleation that lead to early tube breaking was also observed even for SWCNTs with large tube diameters. This is because large-scale nearly homogeneous incipient defect nucleation is required to achieve large tensile ductility in large CNTs. Otherwise, early defect concentration would lead to the weakening and failure of a small segment of the tube. For this reason, long tubes, regardless of their diameters, are

more prone to such early structural failure under tensile loading. This phenomenon has its roots in the statistical nature of thermal energy that plays a key role in the defect activation. In some of our simulations, the overall elongation behaviors are different in different runs with some being ductile while others more brittle due to stronger defect localization under the same simulation conditions on the same SWCNTs. This situation is similar to what was observed in experiments.[59] For example, in Fig. 2 of Ref. 9, a CNT was observed to break soon after being pulled at high temperature, exhibiting a brittle breaking mode. In a recent simulation on tensile loading of copper nanowires, it was found that both the breaking modes and locations of a Cu nanowire can be completely different at the same strain rate,[35] which is similar to the results for SWCNTs obtained in our simulations.

IV. CONCLUDING REMARKS

In summary, by extensive large-scale molecular dynamics simulations, we reveal that tensile ductility exists in SWCNTs with large [above that of the (31,0) tube] diameters over a wide temperature range between 500 and 2400 K. Reduction in thermal energy at lower temperatures impedes defect activation and motion and leads to brittle breaking modes under tensile loading. For SWCNTs with smaller diameters, strong localization of incipient defects result in brittle tensile breaking modes even at high temperatures. The interplay of thermal and strain energy responsible for defect nucleation and motion leads to an almost linear increase of the elastic limit of SWCNTs with decreasing temperature. On the basis of this observation and consideration of the Joule heating procedure employed in recent experiments, we propose and demonstrate a self-enhancing plastic elongation mechanism for SWCNTs via temperature modulation during the elongation process by a slight temperature reduction beyond the elastic limit. Our simulation results resemble the experimentally observed superelongation of carbon nanotubes at high temperatures and suggest their tensile deformation behavior over a wide temperature range for tubes with different diameters. These results add to a systematic understanding of this intriguing phenomenon which may have broad implications for similar tensile deformation in other nanostructures.

It should be mentioned that several aspects concerning the experimentally observed CNT superelongation deserve further investigation. The atomistic mechanism of apparent mass loss at elevated temperatures and its role in the superplastic tensile elongation process requires additional work, although our reported simulations indicate that it is not essential for the superplastic behavior of CNTs. The transition between armchair and zigzag CNTs in realistic large-scale tubes at high temperatures is also an unsettled and interesting issue. The strain rate in the present study is much higher than that in the experiments of Huang *et al.*,[8,9] which is expected to have a major influence on the physics. Considering that strain rates in realistic processes under diverse loading conditions could be either faster or slower,[8,9,60] a closer examination of the effect of faster or slower strain rate on some of these processes may offer further insight into the detailed dislocation dynamics that could have important implications. Efforts to resolve these issues are expected to lead to a more comprehensive understanding of structural deformation of CNTs and are, therefore, highly desirable.

ACKNOWLEDGMENTS

We acknowledge useful communications with Jianyu Huang regarding some experimental results. This work was supported by DOE under Cooperative Agreement No. DE-FC52-06NA26274 (C.T. and C.F.C.), by 973 Program (Contract No. 2007CB936204), by NSFC (Contract No. 10732040), and by MOE of China (W.L.G.). C.T. was also supported by the Innovative Ph.D. thesis fund of NUAA (Contract No. 4003-019015).

[1] K. Koziol, J. Vilatela, A. Moisala, M. Motta, P. Cunniff, M. Sennett, and A. Windle, Science **318**, 1892 (2007).
[2] M. Treacy, T. Ebbesen, and J. Gibson, Nature (London) **381**, 678 (1996).
[3] M. F. Yu, O. Lourie, M. J. Dye, K. Moloni, T. F. Kelly, and R. S. Ruoff, Science **287**, 637 (2000).
[4] Q. Zhao, M. Buongiorno Nardelli, and J. Bernholc, Phys. Rev. B **65**, 144105 (2002).
[5] T. Belytschko, S. P. Xiao, G. C. Schatz, and R. S. Ruoff, Phys. Rev. B **65**, 235430 (2002).
[6] D. A. Walters, L. Ericson, M. Casavant, D. Colbert, K. Smith, and R. E. Smalley, Appl. Phys. Lett. **74**, 3803 (1999).
[7] M. F. Yu, B. S. Files, S. Arepalli, and R. S. Ruoff, Phys. Rev. Lett. **84**, 5552 (2000).
[8] J. Y. Huang, S. Chen, Z. Q. Wang, K. Kempa, Y. M. Wang, S. H. Jo, G. Chen, M. S. Dresselhaus, and Z. F. Ren, Nature (London) **439**, 281 (2006).
[9] J. Y. Huang, S. Chen, Z. F. Ren, Z. Wang, K. Kempa, M. J. Naughton, G. Chen, and M. S. Dresselhaus, Phys. Rev. Lett. **98**, 185501 (2007).
[10] M. Buongiorno Nardelli, B. I. Yakobson, and J. Bernholc, Phys. Rev. Lett. **81**, 4656 (1998).
[11] B. I. Yakobson, Appl. Phys. Lett. **72**, 918 (1998).
[12] T. Dumitrica, M. Hua, and B. I. Yakobson, Proc. Natl. Acad. Sci. U.S.A. **103**, 6105 (2006).
[13] P. Zhang, P. E. Lammert, and V. H. Crespi, Phys. Rev. Lett. **81**, 5346 (1998).
[14] F. Ding, K. Jiao, M. Wu, and B. I. Yakobson, Phys. Rev. Lett. **98**, 075503 (2007).
[15] J. Y. Huang, S. Chen, Z. F. Ren, Z. Q. Wang, D. Z. Wang, M. Vaziri, Z. Suo, G. Chen, and M. S. Dresselhaus, Phys. Rev. Lett. **97**, 075501 (2006).
[16] B. I. Yakobson, M. Campbell, C. Brabec, and J. Bernholc, Comput. Mater. Sci. **8**, 341 (1997).
[17] C. Wei, K. Cho, and D. Srivastava, Phys. Rev. B **67**, 115407 (2003).

[18] D. W. Brenner, Phys. Rev. B **42**, 9458 (1990).
[19] D. W. Brenner, S. A. Shenderova, J. A. Harisson, S. J. Stuart, B. Ni, and S. B. Sinnott, J. Phys.: Condens. Matter **14**, 783 (2002).
[20] H. Berendsen, J. Postma, W. Gunsteren, A. DiNola, and J. Haak, J. Chem. Phys. **81**, 3684 (1984).
[21] W. Guo, C. Z. Zhu, T. X. Yu, C. H. Woo, B. Zhang, and Y. T. Dai, Phys. Rev. Lett. **93**, 245502 (2004).
[22] J. A. Elliott, J. K. W. Sandler, A. H. Windle, R. J. Young, and M. S. P. Shaffer, Phys. Rev. Lett. **92**, 095501 (2004).
[23] X. J. Duan, C. Tang, J. Zhang, W. L. Guo, and Z. F. Liu, Nano Lett. **7**, 143 (2007).
[24] S. Iijima, C. Brabec, A. Maiti, and J. Bernholc, J. Chem. Phys. **104**, 2089 (1996).
[25] B. I. Yakobson, C. J. Brabec, and J. Bernholc, Phys. Rev. Lett. **76**, 2511 (1996).
[26] A. Kutana and K. P. Giapis, Phys. Rev. Lett. **97**, 245501 (2006).
[27] X. Y. Li, W. Yang, and B. Liu, Phys. Rev. Lett. **98**, 205502 (2007).
[28] T. Belytschko, S. P. Xiao, G. C. Schatz, and R. Ruoff, Phys. Rev. B **65**, 235430 (2002).
[29] D. Troya, S. Mielke, and G. Schatz, Chem. Phys. Lett. **382**, 133 (2003).
[30] B. P. Uberuaga, S. J. Stuart, and A. F. Voter, Phys. Rev. B **75**, 014301 (2007).
[31] O. A. Shenderova, D. W. Brenner, A. Omeltchenko, X. Su, and L. H. Yang, Phys. Rev. B **61**, 3877 (2000).
[32] S. Zhang, S. L. Meilke, R. Khare, D. Troya, R. S. Ruoff, G. C. Schatz, and T. Belytschko, Phys. Rev. B **71**, 115403 (2005).
[33] E. Kaxiras and K. C. Pandey, Phys. Rev. Lett. **61**, 2693 (1988).
[34] G. D. Lee, C. Z. Wang, E. Yoon, N. M. Hwang, D. Y. Kim, and K. M. Ho, Phys. Rev. Lett. **95**, 205501 (2005).
[35] D. Wang, J. Zhao, S. Hu, X. Yin, S. Liang, Y. Liu, and S. Deng, Nano Lett. **7**, 1208 (2007).
[36] K. M. Liew, X. Q. He, and C. H. Wong, Acta Mater. **52**, 2521 (2004).
[37] J. X. Wei, K. M. Liew, and X. Q. He, Appl. Phys. Lett. **91**, 261906 (2007).
[38] M. Marques, H. Troiani, M. Miki-Yoshida, M. Jose-Yacaman, and A. Rubio, Nano Lett. **4**, 811 (2004).
[39] C. Tang, W. L. Guo, and C. F. Chen, Phys. Rev. Lett. **100**, 175501 (2008).
[40] B. I. Yakobson and R. E. Smalley, Am. Sci. **85**, 324 (1997).
[41] S. Zhang and T. Zhu, Philos. Mag. Lett. **87**, 567 (2007).
[42] G. G. Samsonidze, G. G. Samsonidze, and B. I. Yakobson, Phys. Rev. Lett. **88**, 065501 (2002).
[43] C. Jin, K. Suenaga, and S. Iijima, Nano Lett. **8**, 1127 (2008).
[44] S. Mielke, D. Troya, S. Zhang, J. Li, S. Xiao, R. Car, R. Ruoff, G. Schatz, and T. Belytschko, Chem. Phys. Lett. **390**, 413 (2004).
[45] J. Y. Huang, F. Ding, K. Jiao, and B. I. Yakobson, Phys. Rev. Lett. **99**, 175503 (2007).
[46] F. Ding, K. Jiao, Y. Lin, and B. I. Yakobson, Nano Lett. **7**, 681 (2007).
[47] G. Lee, C. Wang, J. Yu, E. Yoon, N. Hwang, and K. Ho, Appl. Phys. Lett. **92**, 043104 (2008).
[48] G. E. Begtrup, K. G. Ray, B. M. Kessler, T. D. Yuzvinsky, H. Garcia, and A. Zettl, Phys. Rev. Lett. **99**, 155901 (2007).
[49] M. Yang, V. Koutsos, and M. Zaiser, Nanotechnology **18**, 155708 (2007).
[50] S. Fan, M. Chapline, N. Franklin, T. Tombler, A. Cassell, and H. Dai, Science **283**, 512 (1999).
[51] W. Kim, H. Choi, M. Shim, Y. Li, D. Wang, and H. Dai, Nano Lett. **2**, 703 (2002).
[52] H. Guo, P. Yan, Y. Wang, J. Tan, Z. Zhang, M. Sui, and E. Ma, Nature Mater. **6**, 735 (2007).
[53] X. Han, K. Zheng, Y. Zhang, X. Zhang, Z. Zhang, and Z. Wang, Adv. Mater. **19**, 2112 (2007).
[54] Y. Zhang, X. Han, K. Zheng, Z. Zhang, X. Zhang, J. Fu, Y. Ji, Y. Hao, X. Guo, and Z. Wang, Adv. Funct. Mater. **17**, 3435 (2007).
[55] S. Park, D. Srivastava, and K. Cho, Nano Lett. **3**, 1273 (2003).
[56] G. Dereli and B. Sungu, Phys. Rev. B **75**, 184104 (2007).
[57] T. Zhu, J. Li, A. Samanta, A. Leach, and K. Gall, Phys. Rev. Lett. **100**, 025502 (2008).
[58] T. Chang and H. Gao, J. Mech. Phys. Solids **51**, 1059 (2003).
[59] J. Y. Huang (private communication).
[60] J. Kim, T. LaGrange, B. Reed, M. Taheri, M. Armstrong, W. King, N. Browning, and G. Campbell, Science **321**, 1472 (2008).